JGR Atmospheres

RESEARCH ARTICLE
10.1029/2019JD031563

A Scale-Aware Parameterization for Estimating Subgrid Variability of Downward Solar Radiation Using High-Resolution Digital Elevation Model Data

Siwei He[1,2], **Tatiana G. Smirnova**[2,3], **and Stanley G. Benjamin**[2]

[1]National Research Council, Washington, DC, USA, [2]NOAA/OAR/Earth System Research Laboratory/Global Systems Division, Boulder, CO, USA, [3]Cooperative Institute for Research in Environmental Sciences, University of Colorado Boulder, Boulder, CO, USA

Key Points:
- Subgrid variability of downward solar radiation and subgrid variability of terrain are connected in a straightforward way in this study
- The proposed scheme provides an effective approach to include high-resolution topographic information in a coarse model grid cell
- The proposed scheme can be used in any hydrological or land-surface model to estimate variance of downward solar radiation

Correspondence to:
S. He,
siwei.he@noaa.gov

Citation:
He, S., Smirnova, T. G., & Benjamin, S. G. (2019). A scale-aware parameterization for estimating subgrid variability of downward solar radiation using high-resolution digital elevation model data. *Journal of Geophysical Research: Atmospheres*, *124*, 13,680–13,692. https://doi.org/10.1029/2019JD031563

Received 28 AUG 2019
Accepted 18 NOV 2019
Accepted article online 20 NOV 2019
Published online 21 DEC 2019

Author Contributions:
Supervision: Tatiana G. Smirnova, Stanley G. Benjamin
Writing – review & editing: Tatiana G. Smirnova, Stanley G. Benjamin

Abstract Subgrid variability of solar downward radiation at the surface can be important in estimating subgrid variability of other radiation-driven variables, such as snowmelt and soil temperature. However, this information is ignored in current hydrological and weather prediction models as only the mean downward solar radiation of model grid is used. In this study, a parameterization for estimating subgrid variability of downward solar radiation from the model grid mean using high-resolution digital elevation model (DEM) data is proposed. This scheme considers aspect and slope effects on the subgrid variability. The advantage of this scheme is that computations are performed at the same resolution as the considered hydrological or weather prediction model, and subgrid topographic properties derived from high-resolution DEM data are used as static inputs. This proposed scheme has been verified in mountainous and flat areas, respectively. It is found that the scheme can well estimate the subgrid variability of downward solar radiation. Also, effects of the DEM resolution on the calculated subgrid variability and the spatial correlation of downward solar radiation are studied. Results show that modeled subgrid variability highly depends on the resolution of the DEM, while the spatial correlation is negligibly time dependent. The proposed scheme can be used in any hydrological and weather prediction model to estimate subgrid variability of downward solar radiation. For example, it is planned to be tested in future NOAA regional and global weather models to account for the effects of the subgrid variability of downward solar radiation on the snow model of the land-surface component.

1. Introduction

Solar radiation is the energy source for all forms of life, and it determines dynamics of many landscape processes such as transport of soil temperature and moisture, snowmelt, photosynthesis, and transpiration, with direct impact on human society (Hofierka & Suri, 2002). Among others, the spatial variability of solar radiation affects the hydrological cycle and surface energy budget. For example, it affects snowmelt rate, and this contributes to the spatial variability of snow distribution (He et al., 2019). Further, the spatial variability of snow distribution results in differences in surface energy fluxes, which can potentially affect the vertical structures and mixing processes in the atmospheric boundary layer (Wu et al., 2015).

The subgrid variability issue is common in Earth-system models at almost any spatial resolution. Recently, the hydrology community identified 23 unsolved scientific problems in hydrology, and four of them are related to spatial variability and scaling (Blöschl et al., 2019). Generally, a common basic assumption in Earth-system models is that state variables and processes are uniform within a model grid, which is determined by the spatial resolution (Yano, 2016). However, elements of the Earth system are generally heterogeneous and the part of spatial variability within a model grid, referred to as subgrid variability, still could be substantial. Basically, two long-established approaches are used in the practice for representing subgrid variability. One is the statistical dynamic approach (e.g., Avissar, 1992; Liang et al., 1996), and the other is the mosaic approach (e.g., Avissar & Pielke, 1989; Smirnova et al., 2016). In general, the spatial resolution of atmospheric and land-surface models ranges from 1 km to tens of kilometers for different applications. For example, the NOAA operational hourly updated numerical weather prediction systems, the Rapid Refresh and High-Resolution Rapid Refresh, are implemented at the 13- and 3-km spatial resolution, respectively (Benjamin et al., 2016). The National Water Model, which is an operational hydrological model that

simulates and forecasts streamflow over the entire continental United States, runs at a spatial resolution of 1 km (https://water.noaa.gov/about/nwm). Even a spatial resolution of a few kilometers is considered as high resolution in these applications, it is still too coarse to fully capture effects of surface heterogeneity. For instance, land hydrology depends on surface morphology and soil characteristics that can be highly variable in space down to extremely fine scales of a few meters (Giorgi & Avissar, 1997).

The subgrid variability of downward solar radiation can be useful as long as such information is provided for each model grid cell since variabilities of other processes (e.g., snowmelt, evaporation, and soil temperature) affected by solar radiation may be estimated from it. For example, He and Ohara (2019) proposed a model for representing subgrid variability of snow, and the subgrid variability of downward solar radiation information is needed in the model. At the subgrid scale, heterogeneity of downward solar radiation can be remarkable as solar irradiance is dramatically modified by rough topography. Although effects of topography on the downward solar radiation have been well formulated (Bras, 1990; Lee, 1963; Linke, 1922; Sproul, 2007) at point scale, subgrid topographic influences are usually simplified or neglected in hydrological and land-surface models, and only model grid-cell mean values are used. However, an increasing number of studies have found that the subgrid topographic effects on downward solar radiation need to be considered for large-scale applications (Dubayah et al., 1990; Essery & Marks, 2007; He & Ohara, 2019; Helbig & Löwe, 2012; Lai et al., 2010; Lee et al., 2011). These applications include weather-prediction models (e.g., NOAA High-Resolution Rapid Refresh and Rapid Refresh models; Benjamin et al., 2016) where requirements for accurate near-surface predictions necessitate subgrid-scale effects of topography. Therefore, to maintain computation performance, it is necessary to have a parameterization scheme that can efficiently estimate subgrid variability of downward solar radiation from topographic properties of the model grid. Such a scheme is proposed in this study. Topographic properties become more available with the development of new measurement techniques. For example, one-third arc-second digital elevation model (DEM) data of the continental United States (CONUS) can be freely accessed online (https://www.usgs.gov/core-science-systems/ngp/tnm-delivery/), and topographic properties can be computed easily from these DEM data.

There are some studies that have looked at subgrid variability of downward solar radiation (Dubayah et al., 1990; Essery & Marks, 2007; Helbig & Löwe, 2012; Lai et al., 2010; Löwe & Helbig, 2012; Müller & Scherer, 2005), but they focus on estimating model grid-cell mean rather than variance of downward solar radiation within a model grid cell. Dubayah et al. (1990) derived two equations for estimating mean and variance of direct solar radiation by assuming a constant terrain slope and uniformly distributed aspect. However, these assumptions are too limiting and may lead to substantial errors in the weather prediction application on the regional and global scales. Müller and Scherer (2005) proposed a subgrid-scale parameterization scheme computing mean of radiation fluxes for a model grid cell by considering topography at fine resolution. With this method, mean downward solar radiation of the model grid cell can be estimated more accurately compared to Dubayah et al. (1990), but they did not compute the variance within a model gird cell, and also, they did not separate time-dependent variables from static variables. Essery and Marks (2007) developed parameterizations for spatial averages, standard deviations, and distributions of direct and diffuse downward solar radiation with the assumption of fitted Laplace and extreme-value distributions of slope components and horizon angles. Helbig and Löwe (2012) presented a complete radiation parameterization scheme accounting for shading, limited sky views, and terrain reflections in radiation estimation, but they used the scheme of Dubayah et al. (1990) for estimating mean of direct solar radiation with the limitations mentioned above. All these studies focus more on representing grid-cell mean downward solar radiation but give less attention to computing variance of downward solar radiation within a model grid derived from the actual topography.

The purpose of this study is to develop a parameterization scheme to compute variability of downward solar radiation in a model grid cell using the high-resolution DEM data of the model grid cell. More specifically, we establish a relationship between subgrid variability of downward solar radiation and subgrid variability of terrain. The advantage of using the subgrid variability of terrain is that these properties are time independent, can be treated as static inputs, and would not cause additional computation cost in application. We will investigate how subgrid slope and aspect variability control the variability of downward radiation. Also, effects of the spatial resolution of the DEM data on the calculated subgrid variability of downward solar radiation will be evaluated. Finally, the spatial correlation of downward solar radiations will be investigated using the proposed scheme through spatial autocorrelation function (ACF).

This paper has five sections: introduction, methods, results, discussion, and conclusions. Section 2 gives a detailed explanation on the proposed parameterization scheme and a short description of a sophisticated solar radiation model that provides verification on the proposed scheme. Section 3 describes results of this study. Discussion and conclusions are presented in sections 4 and 5, respectively.

2. Methods

2.1. Subgrid Variability of Direct Irradiance

Generally, solar radiation is composed of three components: direct radiation, diffuse radiation, and reflected radiation. These three components have different characteristics. As mentioned by Dubayah et al. (1990), variations in the diffuse and reflected irradiance make relatively little contribution to the overall variability as compared with variability in the direct irradiance. Thus, only the variability from the direct irradiance is considered in this study, and the variabilities of diffuse and reflected radiation are ignored.

The direct irradiance on a plane normal to the direct beam, I_n, can be calculated as (Bras, 1990; Linke, 1922)

$$I_n = W_0 \exp(-T_L a_1 m), \tag{1}$$

where W_0 is the solar constant (1,367 W/m^2), T_L is the Linke atmospheric turbidity coefficient, m is air mass, and a_1 is the Rayleigh optical thickness of air mass m. The direct irradiance on a panel of arbitrary slope and aspect, I_D, is given by

$$I_D = I_n \cos\theta, \tag{2}$$

where I_n is surface direct irradiance from equation (1) (W/m^2) and θ is angle of incidence of the direct irradiance onto the panel surface. From the solar geometric relationships (Sproul, 2007),

$$\begin{aligned} \cos\theta &= \sin(\beta)\sin(\gamma)C_1 + \sin(\beta)\cos(\gamma)C_2 + \cos(\beta)C_3 \\ \text{with} \quad C_1 &= \cos(\alpha_s)\,\sin(\gamma_s) \\ C_2 &= \cos(\alpha_s)\,\cos(\gamma_s) \\ C_3 &= \sin(\alpha_s) \end{aligned}, \tag{3}$$

where β is slope of the panel, γ is aspect of the panel (North is zero and is measured positive to the East), α_s is elevation angle of the Sun, and γ_s is azimuth (aspect) angle of the Sun. Substituting equations (1) and (3) into (2) gives

$$I_D = W_0 \exp(-T_L a_1 m)[\sin(\beta)\sin(\gamma)C_1 + \sin(\beta)\cos(\gamma)C_2 + \cos(\beta)C_3]. \tag{4}$$

This is the equation calculating direct irradiance on a panel of arbitrary slope β and aspect γ with the given Sun's position α_s and γ_s.

Next, we derive an equation for calculating the mean of direct irradiance at a model grid cell by considering the subgrid variability of topography. It is assumed that a model grid cell area consists of many subgrid areas, and direct irradiance at subgrid scale can be calculated through equation (4). If slope, aspect, and direct irradiance of subgrid area i are denoted as β_i, γ_i, and $I_{D,i}$, respectively, the mean direct irradiance, $\bar{I}_D$, of the model grid cell area can be calculated as

$$\bar{I}_D = \langle I_{D,i} \rangle = \langle W_0 \exp(-T_L a_1 m)(\sin(\beta_i)\sin(\gamma_i)C_1 + \sin(\beta_i)\cos(\gamma_i)C_2 + \cos(\beta_i)C_3) \rangle \tag{5}$$

where $\langle\rangle$ is the ensemble-average operator. To simplify equation (5), it is assumed that the Linke atmospheric turbidity coefficient T_L, Rayleigh optical thickness a_1, air mass m, and the Sun's position parameter C_1, C_2, and C_3 are homogeneous within the model grid cell area. This should be a reasonable assumption since the atmospheric conditions and position parameters of the Sun have small variation over distances of order of magnitude of 10 km. Also, this assumption will be verified in section 3.1. Then, equation (5) can be simplified as

$$\text{with}\quad \begin{aligned} \bar{I}_D &= I_n\left(\langle A_{1,i}\rangle C_1 + \langle A_{2,i}\rangle C_2 + \langle A_{3,i}\rangle C_3\right) \\ A_{1,i} &= \sin\beta_i \sin\gamma_i \\ A_{2,i} &= \sin\beta_i \cos\gamma_i \\ A_{3,i} &= \cos\beta_i \end{aligned} \tag{6}$$

This equation calculates the mean direct irradiance of a model grid cell including effects of the subgrid variability of slope and aspect within it. To apply this equation to a model grid, central latitude of the grid, date, local time, and subgrid DEM data should be provided. The verification of this equation is presented in section 3.1. From the above equation, the coefficient for mean, C_m, is defined here as $C_m = (\langle A_{1,i}\rangle C_1 + \langle A_{2,i}\rangle C_2 + \langle A_{3,i}\rangle C_3)$ in this paper for later discussion.

To quantify the variability of direct irradiance within a model grid cell, an equation for calculating variance of direct irradiance is derived as well. We can write subgrid topographic related values in the Reynolds decomposition forms as

$$\begin{aligned} A_{1,i} &= A'_{1,i} + \langle A_{1,i}\rangle \\ A_{2,i} &= A'_{2,i} + \langle A_{2,i}\rangle \\ A_{3,i} &= A'_{3,i} + \langle A_{3,i}\rangle \end{aligned}. \tag{7}$$

These equations decompose each subgrid area value into a model grid-cell mean term and a subgrid fluctuation term. The first term on the right-hand side of equation (7) is the fluctuation term, and the second term on the right-hand side of equation (7) is the model grid-cell mean term. Then, we have

$$\text{with}\quad \begin{aligned} \mathrm{var}(I_D) &= \left\langle \left(I_{D,i} - \bar{I}_D\right)^2 \right\rangle = I_n^2 \left\langle \left(C_1 A'_{1,i} + C_2 A'_{2,i} + C_3 A'_{3,i}\right)^2 \right\rangle = I_n^2 C_v \\ C_v &= C_1^2 \left\langle A'^2_{1,i} \right\rangle + C_2^2 \left\langle A'^2_{2,i} \right\rangle + C_3^2 \left\langle A'^2_{3,i} \right\rangle + 2C_1C_2 \left\langle A'_{1,i} A'_{2,i} \right\rangle + \cdot \\ &\quad 2C_1C_3 \left\langle A'_{1,i} A'_{3,i} \right\rangle + 2C_2C_3 \left\langle A'_{2,i} A'_{3,i} \right\rangle \end{aligned} \tag{8}$$

This equation calculates variance of direct irradiance of a model grid cell by considering subgrid variability of aspect and slope. From equation (8), we can see that the variance of downward solar direct irradiance is a linear combination of variances (the first three terms of C_v) and covariances (the last three terms of C_v) of the subgrid topographic information. The required information for applying this equation is the same as for equation (6), namely, central latitude of the model grid, date, local time, and subgrid DEM data. From equation (8), the coefficient for variance, C_v, is also defined here in this study for later discussion. This equation is useful since it tells us that the spatial variability of downward solar direct radiation can be calculated from the variance and covariance of subgrid topographic information, which is time independent. Time independence means that these values need to be calculated only once and can be treated as static inputs. The shadowing effect was not included in equation (8) although it would be complete to include the process (e.g., Li & Weng, 1988). The reasons are (1) the incoming solar radiation is heavily attenuated when the Sun is low enough for shadowing to occur (Dubayah et al., 1990) and (2) shadowing is time dependent and has to be estimated at the subgrid scale at every time step, increasing computation cost significantly.

In hydrological and land-surface models, the radiation forcing provides the grid-cell mean downward solar radiation, I_D (equation (6)), rather than the direct solar irradiance I_n. Therefore, to estimate the variance of the downward solar radiation from the given grid-cell mean, we can substitute equations (6) into (8) and obtain

$$\mathrm{var}(I_D) = \bar{I}_D^2 \frac{C_v}{C_m^2}. \tag{9}$$

Equation (9) is ready to be used in any hydrological and land-surface models for estimating subgrid variability of downward solar radiation in a model grid cell from the provided mean downward solar radiation of the model grid. The interaction of solar radiation with surface is determined by two groups of factors:

time-dependent parameters (declination angle and solar hour angle) and time-independent parameters (elevation, surface slope and aspect, and latitude). In equation (9), the time-dependent coefficients are evaluated at the model grid cell scale at every time step. The time-independent subgrid terrain properties are computationally intensive, but they are preprocessed and treated as static inputs.

2.2. Solar Radiation Model *r.sun*

In order to verify the proposed parameterization scheme of this study, results of a sophisticated solar radiation model called *r.sun* were used to compare against results of the proposed scheme. *r.sun* is a Geographic Information System-based model, and it is based on previous work done by Hofierka (1997) and implemented in the GRASS® Geographic Information System environment (Neteler & Mitasova, 2013). This model considers the spatial variation of downward solar radiation due to terrain and terrain-shadowing effects, and it can calculate direct, diffuse, reflected, and total solar irradiance (Hofierka & Suri, 2002). Its applicability has been demonstrated in many applications (e.g., Hofierka & Kaňuk, 2009; Nguyen & Pearce, 2010; Pintor et al., 2015; Ruiz-Arias et al., 2009; Šúri & Hofierka, 2004). The algorithm of *r.sun* is described in the paper by Hofierka and Suri (2002). The fundamental required input data of *r.sun* are DEM data.

Model *r.sun* calculates solar radiation based on the resolution of DEM data. For example, if the resolution of the provided DEM data is 50 m, then solar radiation at every 50 m pixel is calculated based on the time, location, and Sun's position. By providing high-resolution DEM data to model *r.sun*, mean and variance of solar radiation over a specific region can be calculated based on the high-resolution solar radiation from model *r.sun*. This method is different from the proposed scheme of this study. The proposed scheme does not calculate solar radiation directly from the provided resolution of the DEM data but calculates coefficients for mean C_m and variance C_v (i.e., from equations (6) and (8)) from the provided resolution of the DEM data. It then calculates mean and variance of solar radiation over the specific region from these two coefficients, time, location, and Sun's position.

3. Results

3.1. Verification

To verify these derived equations for calculating mean (equation (6)) and variance (equation (8)) of downward direct irradiance, comparisons to model *r.sun* have been conducted (Figure 1). Although shading effect is not included in the proposed scheme, it is considered in model *r.sun* for all verifications. Two grids, one from a mountainous area and another from a flat area and both covering 13 km × 13 km at 50 m spatial resolution, have been used in this study for testing and analyzing. Table 1 gives the basic elevation statistical information of these two grid cells, referred to in the following discussion as Grid 1 (mountains) and Grid 2 (flat). From the statistics of Table 1, it can be seen clearly that Grid 1 has more variation in elevation than Grid 2, and this motivates the choice of these two grid cells.

First, mean and variance of downward direct solar irradiance of Grids 1 and 2 have been calculated through the proposed scheme (equations (6) and (8)) and verified by comparing to values computed through model *r.sun*. To make results of these two methods comparable, exactly the same parameters (refer to Hofierka & Suri, 2002) as in model *r.sun* were used in calculating I_n, which is direct irradiance on a horizontal panel given in equation (1). In calculating the Sun's position parameters, latitudes of center points of Grids 1 and 2 (see Table 1) have been used. The topographic trigonometric variables at subgrid scale ($A_{1,i}$, $A_{2,i}$, and $A_{3,i}$) were computed using equation (6). Then, the mean ($\langle A_{1,i}\rangle$, $\langle A_{2,i}\rangle$, and $\langle A_{3,i}\rangle$), variance ($\left\langle A_{1,i}^{'2}\right\rangle$, $\left\langle A_{2,i}^{'2}\right\rangle$, and $\left\langle A_{3,i}^{'2}\right\rangle$), and covariance ($\left\langle A_{1,i}^{'}A_{2,i}^{'}\right\rangle$, $\left\langle A_{1,i}^{'}A_{3,i}^{'}\right\rangle$, and $\left\langle A_{2,i}^{'}A_{3,i}^{'}\right\rangle$) of these trigonometric variables were calculated on a grid scale for both grids. With these calculated grid-scale I_n and topographic mean, variance, and covariance, the mean and variance of downward direct solar irradiance were calculated for Grids 1 and 2 through equations (6) and (8). To validate results from proposed scheme, the mean and variance of downward direct solar irradiance for Grids 1 and 2 were also calculated through subgrid scale values from model *r.sun*. These calculations were performed for every hour on four different days. These four days were selected from winter (1 January, Julian day = 1), spring (1 April, Julian day = 91), summer (1 July, Julian day = 182), and fall (1 October, Julian day = 274). Comparisons of results from the proposed scheme and model *r.sun* are given in Figure 1 and Table 2. The results from the proposed scheme are marked with solid line, and

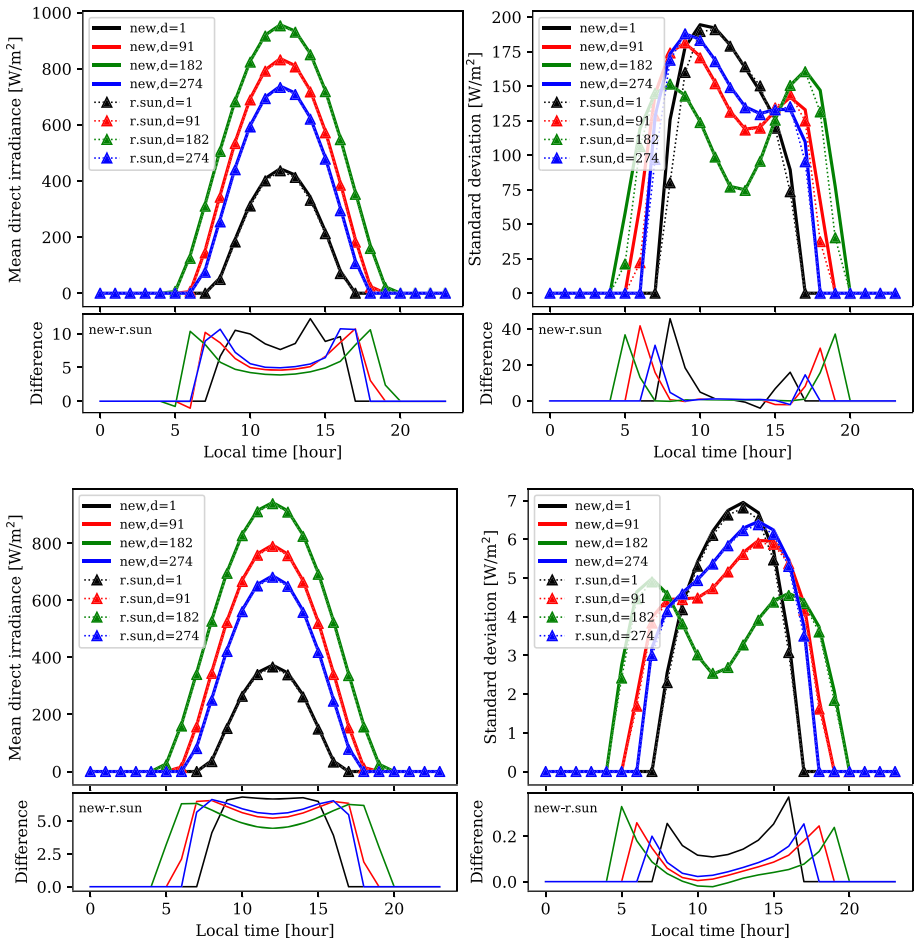

Figure 1. Comparisons of the calculated mean (left) and standard deviation (right) of downward direct solar irradiance from the proposed scheme (i.e., equations (6) and (8)) and model *r.sun*. Results from model *r.sun* are denoted with dash lines with triangle markers, and results from the proposed scheme were denoted with solid lines. Different days are in different colors. The top panel is from the mountainous area (Grid 1), and the bottom panel is from the flat area (Grid 2) at the locations shown in Table 1. The differences between the proposed scheme and model *r.sun* are plotted as the subplots at the bottom of each panel.

the results from the model *r.sun* are marked with triangles. In Table 2, Nash-Sutcliffe Efficiency (e.g., He et al., 2019), which ranges from negative infinity to 100%, is used as the index for evaluating the similarity of the results between the proposed scheme of this paper and the model *r.sun*. Both Figure 1 and Table 2 show that the results from the two different methods match very well. Also, it shows that the calculated variances from equation (8) are a little bit higher than the calculated variances from the model *r.sun* when the Sun's elevation angle is low.

Table 2 shows that all Nash-Sutcliffe Efficiencies for different days are very large, and some of them even up to 100% (perfect match of two time series), which means the results from the proposed scheme and model *r.sun* are very similar.

Table 1
Elevation Statistics of the Two Grids

NO	From	Range (m)	Mean (m)	Standard deviation (m)	Mean slope (degree)	(Longitude, latitude)
Grid cell 1	Mt. area	1,081	2,645	188.8	15.1	(119.715°W,38.141°N)
Grid cell 2	Flat area	55	1,127	11.5	0.5	(102.165°W,40.843°N)

Table 2
Nash-Sutcliffe Efficiency of the Calculated Mean and Standard Deviation From the Proposed Model and Model r.sun

NO	Day = 1 (%)	Day = 91 (%)	Day = 182 (%)	Day = 274 (%)
Grid 1, mean	99.9	100.0	100.0	100.0
Grid 2, mean	99.9	100.0	100.0	100.0
Grid 1, standard deviation	97.9	97.6	96.6	99.1
Grid 2, standard deviation	99.8	99.8	99.7	99.9

Note. As mentioned in Table 1, Grid 1 is from the mountainous area, and Grid 2 is from the flat area.

In deriving equations (6) and (8), it was assumed that the Linke atmospheric turbidity coefficient T_L, Rayleigh optical thickness a_1, air mass m, and the Sun's position parameters C_1, C_2, and C_3 are homogeneous within the grid cell. This assumption will be verified here through a comparison of the spatial distribution of downward solar irradiance with and without the assumption. Spatial distribution of downward direct solar irradiance at subgrid scale is calculated using equation (4), which includes this assumption. On the contrary, model *r.sun* calculates the spatial distribution of downward direct solar irradiance at subgrid scale without making this assumption. Maps and histograms of the spatial distribution of downward solar radiation and the difference for Grids 1 and 2 at 14:00 (local time) on 1 April (day = 91) are shown in Figure 2. This figure demonstrates that the calculated spatial distribution of downward direct solar irradiance from equation (4) is very similar to the one from the model *r.sun* (e.g,, Figures 2a and 2b for Grid 1). Also, both results show clearly that downward solar radiation in the mountainous grid is more heterogeneous than the flat grid. Maps and histograms of total radiation (sum of direct, diffuse, and reflected radiation) from the model *r.sun* are also presented in Figure 2 for later discussion.

The proposed scheme has been also compared against the previous method from Dubayah et al. (1990), and results are given in Figure 3 for different seasons. In this figure, results from model *r.sun* are also marked with triangles and treated as reference values. The results show that the method from Dubayah et al. (1990) overestimates standard deviation when the Sun's elevation angle is relatively high, while the method from this study has improved performance over that from Dubayah et al. (1990).

The proposed scheme does not take into account shadowing effects, and the impact of this limitation has been evaluated using simulations from the model *r.sun*. The results from the *r.sun* simulations with and without shadowing effect for Grid Cell 1 (Table 1) at different dates (Figure 4) show that ignoring shadowing effect causes some errors in calculated variability (standard deviation) of radiation within the grid cell. However, the errors are still relatively small compared to the total variability.

These results lead us to conclude that equations (6) and (8) are accurate enough to study the subgrid variability of solar radiation, and further discussions are presented in section 4.

3.2. DEM Data Resolution Effects on the Subgrid Variability

To investigate effects of DEM data resolution on the calculated subgrid variability of downward solar radiation, mean and variance of solar direct irradiance have been calculated at different resolutions for Grids 1 and 2. Since downward direct irradiance I_n on a horizontal surface is homogeneous within a model grid, only the coefficients for mean and variance have been calculated and analyzed in this section. The coefficient for mean and the coefficient for variance have been defined from equations (6) and (8). One advantage of these coefficients is that they are normalized by the magnitude of solar irradiance and can be compared with each other. However, they are time dependent. In this study, coefficients have been calculated at 8:00, 10:00, 12:00, 14:00, and 16:00 local time on 1 April (day = 91) to investigate effects of the DEM resolution on the subgrid variability. For this purpose, the resolution of DEM data is decreased from 10 to 1,000 m in 20-m increments, and the results are shown in Figure 5. From these results, we can see that (1) effects of resolution on the calculated subgrid variability of downward direct solar irradiance is time dependent; (2) the effect of resolution on the calculated subgrid variability of downward direct solar irradiance is much larger than for the calculated mean; (3) the resolution is longer important for variance (C_v) in the mountainous Grid 1, than in the flat Grid 2; (4) the calculated coefficient for variance (C_v) decreases exponentially with the decrease of spatial resolution, while the coefficient for mean (C_m) changes slightly only in the mountainous Grid 1 due to differences in representation of terrain slope and aspect at different resolutions of DEM data; and (5) for a specific grid, the effect of time of the day on the variability of solar irradiance is less important than topography.

3.3. Spatial Correlation of the Downward Direct Solar Irradiance

Spatial correlation of downward solar irradiance will be studied in this section using the spatial ACF. Dubayah et al. (1990) studied the spatial correlation of downward solar radiation using semivariograms. However, the magnitude of the semivariogram depends on the magnitude of the data. This makes it

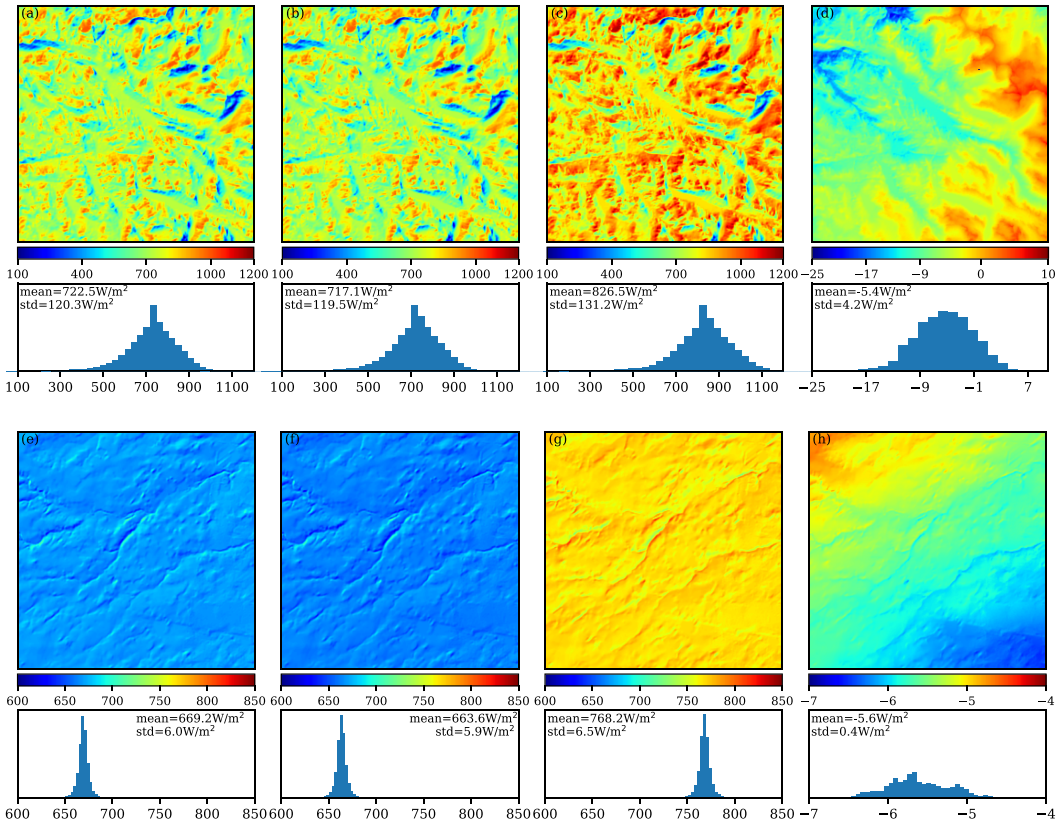

Figure 2. Comparisons of the calculated spatial distribution of downward direct solar irradiance and their histograms from equation (4) and the model *r.sun*. The top panel is from the mountainous area (Grid 1), and the bottom panel is from the flat area (Grid 2). (a) and (e) are downward direct solar irradiance from equation (4), (b) and (f) are downward direct solar irradiance from the model *r.sun*, (c) and (g) are total (sum of direct, diffuse, and reflected) solar irradiance from model *r.sun*, (d) and (h) are difference of downward direct solar irradiance between equation (4) and model *r.run* (i.e., (b) − (a) and (f) − (e)). These values are for 14:00 (local time) on 1 April (day = 91), again using locations in Table 1.

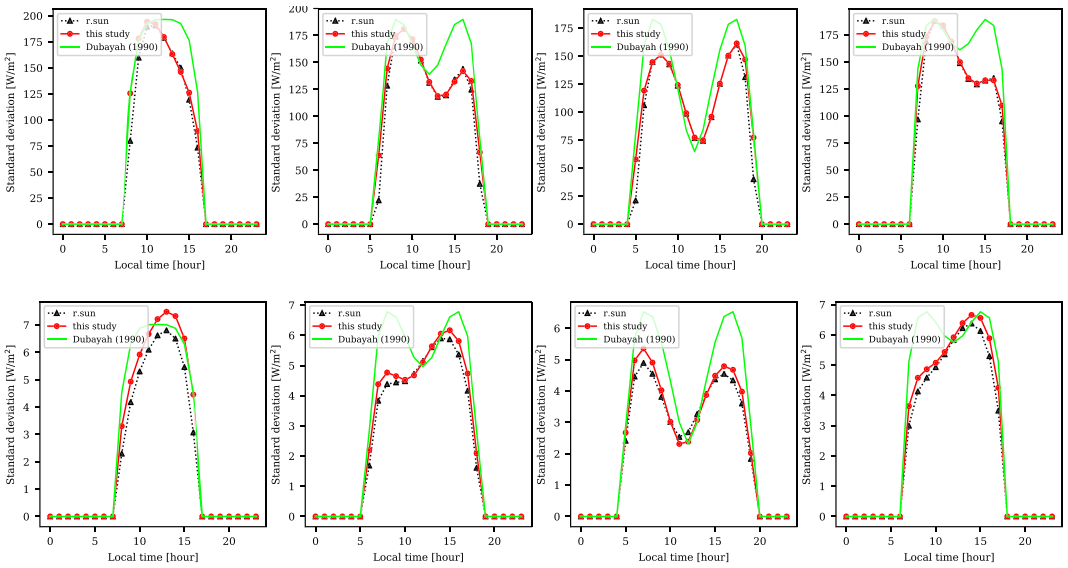

Figure 3. Comparison of the calculated standard deviations between the proposed scheme of this study (red lines) and Dubayah et al. (1990) (green lines). Results from model *r.sun* are also shown in black lines and treated as reference values. The top panel is from the mountainous area (Grid 1), and the bottom panel is from the flat area (Grid 2) at the locations shown in Table 1. From left to right, the corresponding dates are 1 January, 1 April, 1 July, and 1 October.

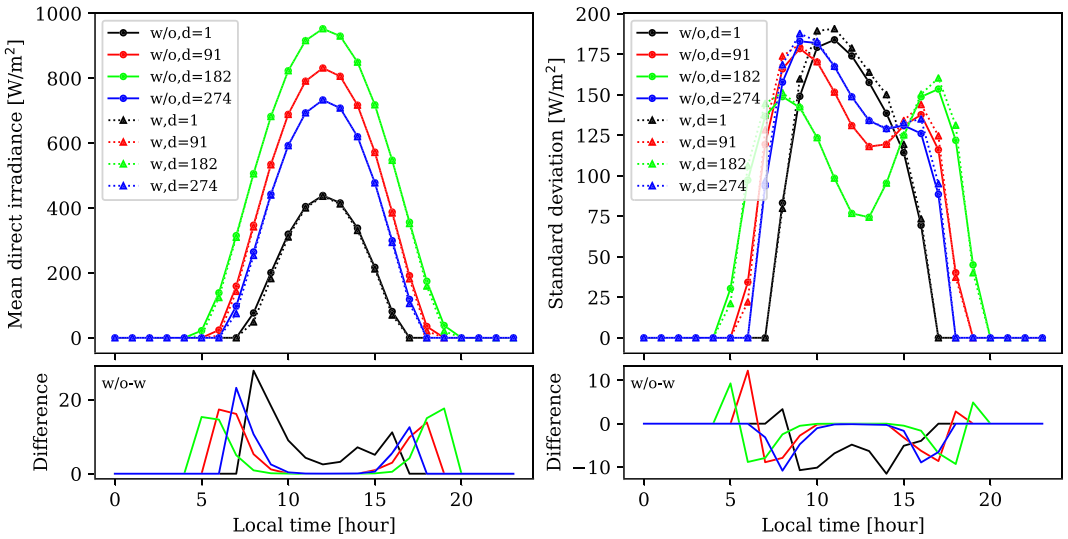

Figure 4. Comparison of (mean = right and standard deviation = left) solar radiation with (dashed lines) and without (solid lines) shadowing effect from *r.sun* model for mountainous Grid 1 (Table 1). Lower panels show the differences between results with and without shadowing effect. Different colors represent days from different seasons (black = 1 January, red = 1 April, green = 1 July, and blue = 1 October).

difficult to compare the calculated semivariogram curves at different times even for the same grid. ACF is a normalized function (Box et al., 2015); therefore, using it to study the spatial correlation of downward solar radiation at different times is more convenient than using a semivariogram. ACFs of downward direct solar irradiance are calculated at five different local times (8:00, 10:00, 12:00, 14:00, and 16:00) on Day 91 for Grids 1 and 2 in 50 m increments up to 5 km, and the results are given in Figure 6. These results demonstrate that

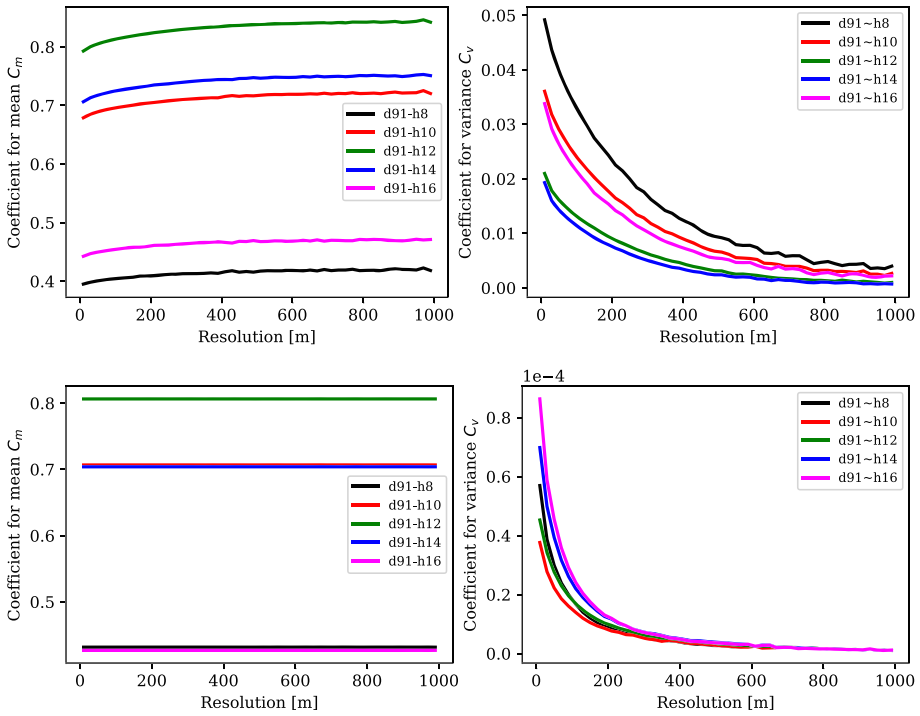

Figure 5. The calculated coefficients for mean (C_m) and variance (C_v) (both are defined in equations (6) and (8)) at different spatial resolutions of DEM data. They are calculated for 8:00, 10:00, 12:00, 14:00, and 16:00 local time (shown in different colors) on Day 91 (1 April). The top panel is from the mountainous area (Grid 1), and the bottom panel is from the flat area (Grid 2).

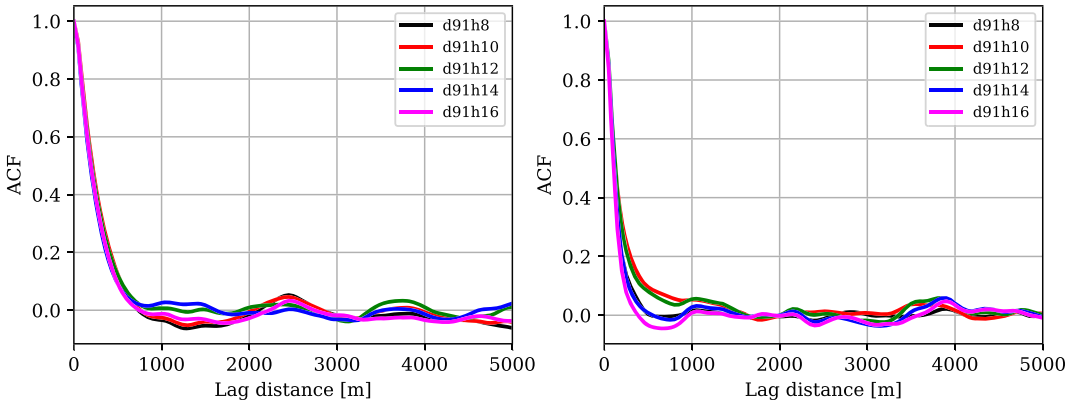

Figure 6. Autocorrelation functions (ACFs) of downward direct solar irradiance at different times shown in different colors on Day 91. The left panel is from the mountainous area (Grid 1), and the right panel is from the flat area (Grid 2).

ACFs of downward direct solar radiation at different times are very similar, and this means that the spatial correlation of downward direct solar irradiance does not change significantly with time. The correlation lengths of Grids 1 and 2 are different as the correlation length varies with topography. From Figure 6, it can be seen that the correlation length is larger in the mountainous area (Grid 1) than the flat area (Grid 2). More details on the potential usage of spatial correlation is given in section 4.

4. Discussion

The effectiveness of the proposed parameterization scheme (i.e., equations (6) and (8)) has been verified through comparing it against the model *r.sun*, which is a sophisticated solar radiation model, over a mountainous area (Grid 1) and a flat area (Grid 2). The results have demonstrated that the proposed scheme is accurate enough in estimating the mean and variance of subgrid downward direct solar irradiance within a model grid. In deriving the parameterization scheme, it is assumed that direct solar irradiance I_n on a horizontal plane and the Sun's position parameters C_1, C_2, and C_3 are homogeneous within a model grid. This assumption has been verified by comparing the calculated spatial distributions of downward direct solar irradiance using equation (4) against the results of model *r.sun* (Figure 2). Maps and histograms of the calculated spatial distribution of downward direct solar irradiance show that the assumption is reasonable since the results with and without this assumption are almost the same. In validating these assumptions, it can be seen from Figure 1 that the calculated variance from the proposed model is larger than the model *r.sun*. From the equation for calculating variance, we know that two factors contribute to the magnitude of variance/standard deviation. The first factor is the magnitude of downward direct solar irradiance, and the second factor is the variability of downward direct solar irradiance. Ignoring the shadowing effect increases the magnitude of solar radiation, thus increasing the variance. Also, ignoring the shadowing effect reduces the variability of solar radiation, thus reducing the variance. In our results, the magnitude of solar radiation from the new model is larger than that from *r.sun* (as we can see from the left two panels of Figure 1), and the variance is larger as well. This demonstrates that the first factor is dominating over the second one.

The second assumption in this study is that the variance of downward solar radiation can be approximated by the variance of downward direct solar radiation, and contributions from the other two components (diffuse and reflected radiation) are negligible. To verify this assumption, spatial distributions of total downward solar irradiance from model *r.sun* were shown in Figures 2c and 2g. Comparing with the spatial distributions of downward direct solar irradiance (Figures 2a, 2b, 2e, and 2f) and their difference (Figures 2d and 2h), we can see that their variances, spatial distributions, and shapes of histograms are highly similar although their means are different. This illustrates that it is reasonable to assume that the variance of total downward irradiance is dominated by the variance of downward direct solar irradiance. This is also consistent with the findings from Dubayah et al. (1990). In addition, the results clearly show that the variability of solar radiation is much larger in the mountainous area (i.e., Grid 1) than in the flat area (i.e., Grid 2). When the Sun's elevation angle is low, the magnitude of diffuse radiation could be larger than direct radiation, and this may

result in larger variance from diffuse radiation (e.g., Liu & Jordan, 1960). However, effects of variance on the related processes, such as snowmelt, soil moisture, and evaporation, are not significant as the total radiation is fairly small when the Sun is low.

The calculated spatial variability of downward direct solar irradiance depends critically on the resolution of DEM data. Equations (6) and (8) are convenient for studying effects of the resolution on the calculated subgrid variability of downward solar radiation since only the coefficients for mean and variance are needed to be calculated while the magnitude of the real solar irradiance is not needed. Section 3.2 is a good example to demonstrate the capability of these two coefficients. It has been realized that the resolution of DEM data affects the representation of variability on solar radiation. However, there is no specific study on how the calculated variability changes with resolution. In section 3.2, their relationships were investigated with these two coefficients. It is found that the mean does not change much with decrease of resolution, but the variance exponentially decreases with the decrease of resolution. The magnitudes of coefficient for variance reveal that the spatial variability of the downward direct solar radiation is much larger in the mountainous area than in the flat area (see Figure 5). It also has been known that the effects of topography on the variability of solar irradiance depend on time as the variability changes with solar position. In addition, it can be seen that the time effect on the variability of downward solar radiation in the mountain area (i.e., Grid 1) is stronger than in the flat area (i.e., Grid 2) because the terrain varies a lot more in the mountain area.

The subgrid variability of downward solar radiation can be estimated using high-resolution DEM data through equations (8) and (9). The proposed scheme treats those required topography properties as static inputs, which are precalculated from the high-resolution DEM data. The proposed scheme does have some time-dependent parameters, but they are separated from topographic parameters and calculated at the grid scale rather than the subgrid scale. Thus, the computational cost of the proposed scheme is very low. Generally, land-surface and hydrological models have the model grid-cell mean downward surface solar radiation from the atmospheric forcing. The variance of subgrid downward solar radiation can be estimated from the given model grid-cell mean surface solar radiation and other parameters through the derived Equation (9) of this study. This would provide additional information on the downward solar radiation that can be potentially used by other processes in estimating subgrid variability, such as snow melt, evaporation, and soil temperature. Also, the proposed scheme provides an effective way to take high-resolution topographic information into consideration in modeling. This is important in mountain hydrology modeling (de Jong, 2015) and large-domain parameter estimation for hydrological and land-surface models (e.g., Mizukami et al., 2017).

Spatial correlation of the downward direct solar radiation is another important characteristic that is useful in modeling. For example, if the Fokker-Planck equation approach is adopted in representing subgrid variability (e.g., He & Ohara, 2019), then spatial correlation lengths of stochastic variables will be critical in determining the diffusion coefficient. From this study, it is found that spatial correlation of the downward direct solar radiation is difficult to describe quantitatively with a general model. However, ACFs of the downward direct solar radiation have shown that the correlation length is only slightly time dependent (Figure 6). In particular, it is found that time effect on correlation length can be ignored in the mountain area (Grid 1). This characteristic is important as it has good potential to simplify calculations in studying effects of subgrid variability of downward solar radiation on other processes, such as snow melting. Since we have related terrain variability to radiation variability, it is possible to predict spatial correlation of radiation from terrain considerations. However, it is generally time dependent, which means that the spatial correlation needs to be calculated at each time. The abovementioned characteristic, namely, the time effect on correlation length can be ignored in the mountain area, means that only one spatial correlation would be a reasonable approximation for different times.

5. Conclusions

A parameterization scheme for estimating mean and variance of subgrid downward solar irradiance by using high-resolution DEM data is proposed in this study. The spatial distribution of radiation and terrain variability are related in a straightforward way through this scheme. This scheme can also be used to approximately evaluate the variability of subgrid downward solar radiation, which is composed of direct, diffuse, and reflected radiation. The proposed scheme has been applied to two grid cells with the size 13 km × 13 km

for verifying its performance. Results from the proposed scheme were compared against the results from the sophisticated radiation model *r.sun*. These comparisons have shown that the proposed scheme performs very well. The following conclusions have been drawn from this study:

1. In determining spatial variability of solar radiation at scale on the order of magnitude of 10 km, it is reasonable to assume that heterogeneity of direct solar irradiance on a horizontal plane and the Sun's position parameters can be ignored. At this or smaller scale, terrain plays a more important role in affecting downward solar radiation than the others.
2. The subgrid variability of downward solar radiation can be estimated from high-resolution DEM data through the proposed scheme of this study. Although the subgrid variability is time dependent, the proposed scheme of this study will not significantly increase computational cost since the required topography information only needs preprocessing at one time and then is used as a static input. Also, the proposed scheme provides an effective approach to include high-resolution topographic information in model grids.
3. The resolution of the DEM data has big effects on the calculated subgrid variability of the downward solar radiation. The high-resolution DEM data can represent the subgrid variability much better than the coarse-resolution DEM data, and the variance of subgrid downward direct solar radiation exponentially decreases with the decrease of the resolution of the DEM data. Resolution of DEM data does not obviously affect mean of the downward solar radiation. Also, it was found that the effect of time on the variability of solar irradiance decreases with decrease in resolution.
4. The spatial correlation of the downward direct solar radiation obviously varies with topography, but it only slightly changes with time.

The next step is to apply this subgrid variability of solar radiation within a full weather/land-surface prediction model to consider subgrid variability of other radiation-driven processes. For instance, Smirnova et al. (2016) showed that improved representation of subgrid snow processes can result in more accurate 2-m air temperature prediction in such a model. Application of this new parameterization scheme to weather prediction will be described in a subsequent paper.

Acknowledgments
We thank Dr. John M. Brown and Dr. Michael Toy of ESRL/GSD for insightful reviews of this manuscript. We also would like to thank the Editor and anonymous reviewers for their helpful comments and suggestions. This work has been supported under NOAA Research base funding. The data and source codes of this manuscript can be accessed online (https://doi.org/10.5281/zenodo.3380737).

References

Avissar, R. (1992). Conceptual aspects of a statistical-dynamical approach to represent landscape subgrid-scale heterogeneities in atmospheric models. *Journal of Geophysical Research*, *97*(D3), 2729–2742.

Avissar, R., & Pielke, R. A. (1989). A parameterization of heterogeneous land surfaces for atmospheric numerical models and its impact on regional meteorology. *Monthly Weather Review*, *117*(10), 2113–2136.

Benjamin, S. G., Weygandt, S. S., Brown, J. M., Hu, M., Alexander, C. R., Smirnova, T. G., et al. (2016). A North American hourly assimilation and model forecast cycle: The rapid refresh. *Monthly Weather Review*, *144*(4), 1669–1694. https://doi.org/10.1175/MWR-D-15-0242.1

Blschl, G., Bierkens, M. F. P., Chambel, A., Cudennec, C., Destouni, G., Fiori, A., et al. (2019). Twenty-three unsolved problems in hydrology (UPH)—A community perspective. *Hydrological Sciences Journal*, *64*(10), 1141–1158. https://doi.org/10.1080/02626667.2019.1620507

Box, G. E. P., Jenkins, G. M., Reinsel, G. C., & Ljung, G. M. (2015). *Time series analysis: Forecasting and control*. Honokenm, NJ: John Wiley & Sons.

Bras, R. L. (1990). *Hydrology: An introduction to hydrologic science*. Reading: Addison-Wesley.

de Jong, C. (2015). Challenges for mountain hydrology in the third millennium. *Frontiers in Environmental Science*, *3*(38). https://doi.org/10.3389/fenvs.2015.00038

Dubayah, R., Dozier, J., & Davis, F. W. (1990). Topographic distribution of clear-sky radiation over the Konza Prairie, Kansas. *Water Resources Research*, *26*(4), 679–690. https://doi.org/10.1029/WR026i004p00679

Essery, R., & Marks, D. (2007). Scaling and parametrization of clear-sky solar radiation over complex topography. *Journal of Geophysical Research*, *112*, D10122. https://doi.org/10.1029/2006JD007650

Giorgi, F., & Avissar, R. (1997). Representation of heterogeneity effects in Earth system modeling: Experience from land surface modeling. *Reviews of Geophysics*, *35*(4), 413–437. https://doi.org/10.1029/97RG01754

He, S., & Ohara, N. (2019). Modeling subgrid variability of snow depth using the Fokker-Planck equation approach. *Water Resources Research*, *55*, 3137–3155. https://doi.org/10.1029/2017WR022017

He, S., Ohara, N., & Miller, S. (2019). Understanding subgrid variability of snow depth at 1-km scale using Lidar measurements. *Hydrological Processes*, *33*, 1523–1537. https://doi.org/10.1002/hyp.13415

Helbig, N., & Löwe, H. (2012). Shortwave radiation parameterization scheme for subgrid topography. *Journal of Geophysical Research*, *117*, D03112. https://doi.org/10.1029/2011JD016465

Hofierka, J. (1997). *Direct solar radiation modelling within an open GIS environment*." In Proceedings of Jec-Gi'97 Conference in Vienna, Austria (pp. 575–584). Amsterdam: Ios Press.

Hofierka, J., & Suri, M. (2002). "The solar radiation model for Open source GIS: Implementation and applications." In *Proceedings of the Open Source GIS-Grass Users Conference*, 2002:51–70.

Hofierka, J., & Kaňuk, J. (2009). Assessment of photovoltaic potential in urban areas using open-source solar radiation tools. *Renewable Energy*, *34*(10), 2206–2214. https://doi.org/10.1016/j.renene.2009.02.021

Lai, Y.-J., Chou, M.-D., & Lin, P.-H. (2010). Parameterization of topographic effect on surface solar radiation. *Journal of Geophysical Research*, *115*, D01104. https://doi.org/10.1029/2009JD012305

Lee, R.. (1963). Evaluation of solar beam irradiation as a climatic parameter of mountain watersheds. *Hydrology Papers (Colorado State University); No. 2*. Colorado State University. Libraries.

Lee, W.-L., Liou, K. N., & Hall, A. (2011). Parameterization of solar fluxes over mountain surfaces for application to climate models. *Journal of Geophysical Research*, *116*, D01101. https://doi.org/10.1029/2010JD014722

Li, Z., & Weng, D. (1988). A computer model for calculating the duration of sunshine in mountainous areas. *Chinese Science Bulletin*, *33*, 1624–1627.

Liang, X., Lettenmaier, D. P., & Wood, E. F. (1996). One-dimensional statistical dynamic representation of subgrid spatial variability of precipitation in the two-layer variable infiltration capacity model. *Journal of Geophysical Research*, *101*(D16), 21403. https://doi.org/10.1029/96JD01448

Linke, F. (1922). Transmissionkoeflizient und Trubungsfaktor. *Beiträge zur Physik der Atmosphäre*, *10*, 91–103.

Liu, B. Y. H., & Jordan, R. C. (1960). The interrelationship and characteristic distribution of direct, diffuse and total solar radiation. *Solar Energy*, *4*(3), 1–19.

Löwe, H., & Helbig, N. (2012). Quasi-analytical treatment of spatially averaged radiation transfer in complex topography. *Journal of Geophysical Research*, *117*, D19101. https://doi.org/10.1029/2012JD018181

Mizukami, N., Clark, M. P., Newman, A. J., Wood, A. W., Gutmann, E. D., Nijssen, B., et al. (2017). Towards seamless large-domain parameter estimation for hydrologic models. *Water Resources Research*, *53*, 8020–8040. https://doi.org/10.1002/2017WR020401

Müller, M. D., & Scherer, D. (2005). A grid- and subgrid-scale radiation parameterization of topographic effects for mesoscale weather forecast models. *Monthly Weather Review*, *133*(6), 1431–1442. https://doi.org/10.1175/MWR2927.1

Neteler, M., & Mitasova, H. (2013). *Open source Gis: A GRASS GIS approach* (Vol. 689). New York, NY: Springer Science & Business Media.

Nguyen, H. T., & Pearce, J. M. (2010). Estimating potential photovoltaic yield with *r.sun* and the open source Geographical Resources Analysis Support System. *Solar Energy*, *84*(5), 831–843. https://doi.org/10.1016/j.solener.2010.02.009

Pintor, B. H., Sola, E. F., Teves, J., Inocencio, L. C., Ang, M., & Concepcion, R. (2015). Solar energy resource assessment using R. SUN in GRASS GIS and site suitability analysis using AHP for groundmounted solar photovoltaic (Pv) farm in the Central Luzon Region (Region 3), Philippines. In *Free and open source software for geospatial (Foss4g) Conference Proceedings*, 15:3. 1.

Ruiz-Arias, J. A., Tovar-Pescador, J., Pozo-Vázquez, D., & Alsamamra, H. (2009). A comparative analysis of DEM-based models to estimate the solar radiation in mountainous terrain. *International Journal of Geographical Information Science*, *23*(8), 1049–1076. https://doi.org/10.1080/13658810802022806

Smirnova, T. G., Brown, J. M., Benjamin, S. G., & Kenyon, J. S. (2016). Modifications to the rapid update cycle land surface model (RUC LSM) available in the weather research and forecasting (WRF) model. *Monthly Weather Review*, *144*(5), 1851–1865.

Sproul, A. B. (2007). Derivation of the solar geometric relationships using vector analysis. *Renewable Energy*, *32*(7), 1187–1205. https://doi.org/10.1016/j.renene.2006.05.001

Šúri, M., & Hofierka, J. (2004). A new GIS-based solar radiation model and its application to photovoltaic assessments. *Transactions in GIS*, *8*(2), 175–190. https://doi.org/10.1111/j.1467-9671.2004.00174.x

Wu, C.-M., Lo, M.-H., Chen, W.-T., & Chia-Tsung, L. (2015). The impacts of heterogeneous land surface fluxes on the diurnal cycle precipitation: A framework for improving the GCM representation of land-atmosphere interactions. *Journal of Geophysical Research: Atmospheres*, *120*, 3714–3727. https://doi.org/10.1002/2014JD023030

Yano, J.-I. (2016). Subgrid-scale physical parameterization in atmospheric modeling: How can we make it consistent? *Journal of Physics A: Mathematical and Theoretical*, *49*(28), 284001. http://stacks.iop.org/1751-8121/49/i=28/a=284001